Phosphine oxide functionalised with two bipyridine subunits: a novel ligand for the engineering of sterically hindered complexes

Laurent Douce,[a] Loïc Charbonnière,[a] Michèle Cesario[b] and Raymond Ziessel*[a]

[a] *Laboratoire de Chimie, d'Electronique et de Photonique Moléculaires (CNRS UPRESA 7008), ECPM 25, rue Becquerel, F-67087 Strasbourg cedex 2, France. E-mail: ziessel@chimie.u-strasbg.fr*

[b] *Institut de Chimie des Substances Naturelles, CNRS, F-91128 Gif-sur-Yvette, France*

Received (in Montpellier, France) 19th March 2000, Accepted 24th April 2001
First published as an Advance Article on the web 10th July 2001

Ligand **L**, containing two 6-methyl-6′-methyl-yl-2,2′-bipyridine moieties linked by a "PhP=O" spacer, has been prepared. Subsequent complexation with $[Cu(CH_3CN)_4](BF_4)$ led to a unique complex of formula $[Cu\mathbf{L}](BF_4)$. The molecular structure has been determined by X-ray crystallography in the solid state and NMR studies in solution. The complex displays an intense absorption band in the visible wavelength range with maxima at 418 and 509 nm, and is oxidised reversibly at $+0.66$ V ($\Delta E_p = 80$ mV) to the corresponding Cu(II) species, while two successive reductions of the coordinated bipyridine fragments occur at -1.60 ($\Delta E_p = 66$) and -1.84 V ($\Delta E_p = 70$ mV) *vs.* SCE. Direct spectrophotometric titrations with global analysis allowed us to elicit stability constants for the emergent complex and to highlight the formation of a dinuclear complex in the presence of excess copper.

Research to synthesise fascinating molecular structures, often involving interlocking of complementary molecular components, has blossomed during the past decade.[1] Numerous examples have been engineered with the prospect of forming symmetrical and esthetic structures. In several cases cationic metal centres provide the impetus for self-organisation into ordered structures, some of them exhibiting useful catalytic,[2] mesomorphic[3] or electronic properties.[4] Many of the new complexes generated over the last few years rely on the coordination of transition metal cations to polypyridine fragments incorporated into oligomeric ribbons or macroscopic loops.[5–8] By virtue of forming relatively stable and well-defined complexes with metal cations, Lehn and co-workers have led the field by designing linear polybipyridyl ligands that self-organise in the presence of copper(I) cations to form double-stranded helicates.[9] Furthermore, related structures have been constructed using various kinds of oligopyridines and different transition metals such as Cu(II), Co(II), Cd(II) and Zn(II).[10] Specifically, such elaborated molecular architectures are made possible by incorporating several polypyridine units into oligomeric or macrocyclic multitopic ligands. Some attempts have been made to identify the driving forces for the formation of one structure *vs.* another by systematic variation of the metal and ligand component, but very little is known about the mechanism of formation of these complexes.[11]

It is worthwhile pointing out that only a few metal-induced self-assembled structures have been produced with bipyridine-grafted phosphanes.[12] Hybrid ligands, in which a phosphorous(V) is used as a connecting atom, are available[13] but genuine bipyridine–P(V) ligands are very scarce. The aim of the present work is to partially fill this gap and to describe the full characterisation of ligand **L**, its related mononuclear copper(I) complex and to determine its stability constant in solution. The molecular structure of the complex in the solid state was deduced from X-ray crystallographic studies.

One clear advantage of this new ligand is that it can be used in the complexation of a variety of different transition metals and also with lanthanide cations and could readily be functionalised either at the phenyl ring or at the methyl positions.

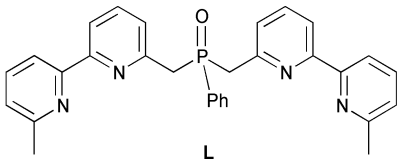

L

This provides the key element by which to include this structure into elaborated complexes and the impetus for constructing macroscopic sensors.

Experimental

General methods

The 200.1, 400.1 (^{1}H), 50.3 (^{13}C) and 162 MHz (^{31}P) NMR spectra were recorded at room temperature, unless otherwise specified, using perdeuterated solvent as an internal standard: δ(H) relative to residual protiated solvent in $CDCl_3$ (7.26); δ(C) relative to the solvent in $CDCl_3$ (77.0). Melting points were obtained on a Büchi 535 capillary melting point apparatus in open-ended capillaries and are uncorrected. FT-IR spectra were measured from KBr pellets with a Nicolet 210 spectrometer. Fast-atom bombardement (FAB, positive mode) mass spectra were obtained using *m*-nitrobenzyl alcohol (*m*-NBA) as the matrix. UV-Vis absorption spectra and spectrophotometric titrations were performed on a Uvikon 933 spectrophotometer using degassed acetonitrile as solvent containing 10^{-3} M tetrabutylammonium hexafluorophosphate as an inert salt. Titrations were performed according to literature procedures[14] with typical concentrations of 5×10^{-5} M for the ligand and 5×10^{-4} M for $[Cu(CH_3CN)_4](BF_4)$.

Electrochemical studies employed cyclic voltammetry with a conventional 3-electrode system using a BAS CV-50W voltammetric analyser equipped with a Pt microdisk working electrode and a Ag wire counter-electrode. Ferrocene was used as an internal standard and was calibrated against a saturated calomel reference electrode (SCE) separated from the electrolysis cell by a glass frit presoaked with electrolyte solution. Solutions contained the electrode-active substrate

 DOI: 10.1039/b102520c

(*ca.* 2×10^{-4} M) in deoxygenated and anhydrous acetonitrile containing tetra-*n*-butylammonium tetrafluoroborate (0.2 M) as supporting electrolyte. The quoted half-wave potentials were reproducible within 20 mV.

Materials

$PhPCl_2$ and $NaIO_4$ are commercially available. 6,6′-Dimethyl-2,2′-bipyridine[15] and $[Cu(CH_3CN)_4](BF_4)$[16] were prepared and purified according to literature procedures. Diisopropylamine and tetrahydrofuran were dried over suitable reagents and freshly distilled under argon before use. All reactions were carried out under dry argon by using Schlenk-tube and vacuum-line techniques.

Synthesis of ligand L. A solution of n-butyllithium in hexane (3.85 mL, 1.5 M, 5.75 mmol) was slowly added to a solution of diisopropylamine (1 mL, 7.13 mmol) in THF (50 mL) at −78 °C. After 0.5 h, solid 6,6′-dimethyl-2,2′-bipyridine (1.059 g, 5.75 mmol) was carefully added to the stirred solution, which immediately turned deep blue–green. The temperature was allowed to rise to room temperature and kept at this temperature for 0.5 h and then cooled to −78 °C for an additional hour. Then, phenyldichlorophosphine (0.39 mL, 2.875 mmol) was slowly added to the solution. Stirring was maintained for 0.25 h and the solution was allowed to warm to room temperature. The resultant yellow solution was evaporated under vacuum and the yellow residue was dissolved in a mixture of dichloromethane and water containing sodium periodate. After stirring for 1 h, the remaining aqueous phase was extracted with dicholoromethane (3 × 50 mL) and the combined organic extracts dried over $MgSO_4$ and evaporated to dryness. The solid was purified by column chromatography on alumina (CH_2Cl_2–hexane: 50 : 50 as eluant) to give 0.75 g of **L** (53%). $C_{30}H_{27}N_4PO$ (M_r = 490.549) Anal. found: C, 73.22; H, 5.29; N, 11.28; calc.: C, 73.46; H, 5.55; N, 11.42%. ^{1}H NMR (200.1 MHz, $CDCl_3$, 25 °C): δ 8.26 (d, 2H, J = 8.7), 7.91 (d, 2H, J = 8.0), 7.63 (m, 6H), 7.31 (m, 5H), 7.12 (d, 2H, J = 7.3), 3.86 [$(AB)_2X$, A = B = H, X = P, 4H, $J_{AB} = J_{AX} = J_{BX}$ = 14.5 Hz], 2.60 (s, 6H, CH_3). $^{13}C\{^1H\}$ NMR (100.61 MHz, $CDCl_3$, 25 °C): δ 158.15 (Cq), 156.42 (d, Cq, J_{PC} = 2), 155.72 (Cq), 152.55 (d, Cq, J_{PC} = 8), 137.80 (d, CH, J_{PC} = 2), 137.24 (CH), 131.94 (d, Cq, J_{PC} = 97), 131.90 (d, CH, J_{PC} = 3), 131.55 (d, CH, J_{PC} = 9), 128.50 (d, CH, J_{PC} = 12), 125.13 (d, CH, J_{PC} = 4), 123.58 (CH), 119.45 (d, CH, J_{PC} = 3), 118.50 (CH), 40.92 (d, CH_2, J_{PC} = 62), 25.01 (CH_3). $^{31}P\{^1H\}$ NMR (162 MHz, $CDCl_3$, 25 °C): δ 36.5 (s). FAB-MS: 491.2 $[M + H]^+$, 475.2 $[M - O + H]^+$. FT-IR (KBr, ν/cm^{-1}): 1577 (s), 1439 (vs), 1185 (m).

Synthesis of copper(I) complex. To a solution of **L** (250 mg, 0.51 mmol) in 15 mL CH_2Cl_2 under argon was added $[Cu(CH_3CN)_4](BF_4)$ (160 mg, 0.51 mmol) in 15 mL CH_3CN. After stirring for 2 h, the deep red solution was evaporated to dryness. Recrystallisation from acetone–hexane yielded red crystals (310 mg, 95%). $C_{30}H_{27}N_4POCuBF_4$ (M_r = 640.900) Anal. found: C, 56.15; H, 4.13; N, 8.69; calc.: C, 56.22; H, 4.25; N, 8.74%. ^{1}H NMR (400.13 MHz, $CDCl_3$, 25 °C): δ 8.52 (d, 1H, H14 bipy), 8.50 (d, 1H, H15 bipy), 8.30 (d, 1H, H5 bipy), 8.21 (d, 1H, H4 bipy), 8.18 (t, 1H, H6 bipy), 8.12 (t, 1H, H16 bipy), 8.02 (t, 1H, H3 bipy), 7.86 (t, 1H, H13 bipy), 7.78 (d, 1H, H7 bipy), 7.60 (t, 1H, $^3J_{HH}$ = 8, H21 phenyl), 7.44 (br m, 4H, H2 + H17 bipy + 2 H20 phenyl), 7.23 (dd, 2H, $^3J_{PH}$ = 11.5, $^3J_{HH}$ = 8, $^4J_{HH}$ = 1.5, 2 H19 phenyl), 6.71 (dd, 1H, ^3J = 8, ^4J = 2, H12 bipy), 4.12 and 3.40 (2H, J_{AB} = 14, $^2J_{AP} = {}^2J_{BP}$ = 18.5, H10 + H11 resp., CH_2), 4.35 and 3.66 (2H, $J_{A'B'}$ = 14, $^2J_{A'P}$ = 18.5, $^2J_{B'P}$ = 8 Hz, H9 and H8 resp., CH_2), 1.92 (s, 3H CH_3), 1.89 (s, 3H, CH_3). $^{31}P\{^1H\}$ NMR (81.01 MHz, $CDCl_3$, 25 °C): δ 37.38 (s). FT-IR (KBr, ν/cm^{-1}): 1596 (s), 1565 (s) 1463 (s), 1439 (s), 1053 (vs br). FAB-MS: m/z 553.3 $[M - BF_4]^+$.

Crystallography

Crystal data for $[CuL](BF_4)$: $C_{30}H_{27}CuN_4POBF_4$, M = 640.88g, triclinic, space group $P\bar{1}$, a = 7.430(3), b = 14.002(5), c = 15.206(6) Å, α = 114.78(2), β = 80.67(3), γ = 98.49(3)°, U = 1411.7(9) Å^3, Z = 2, D_c = 1.508 g cm^{-3}, λ = 0.710 73 Å, T = 293(2) K, μ (Mo Kα) = 0.889 mm^{-1}, $F(000)$ = 656. A prismatic crystal of 0.12 × 0.15 × 0.25 mm was mounted on an Enraf–Nonius Kappa-CCD diffractometer with graphite-monochromated Mo-Kα radiation. The data were collected at room temperature. A full sphere of data was collected by ϕ axis rotation in 2.0° increments over 360°, with 130 s exposures per frame. Dezingering was accomplished by measuring each frame twice. The crystal-to-detector distance was 35 mm. Data were analysed using Kappa-CCD software.[17] Cell dimensions were refined with HKL scalepack.[18] Data reduction was performed with Denzo.[18] Of a total of 18 102 reflections collected, 4975 were independent and 3244 unique reflections were larger than $2\sigma(I)$. The structure was solved by direct methods (SHELXS-86)[19] and refined on F^2 for all reflections by least-squares methods using SHELXL-93.[20] Hydrogen atoms, located by difference syntheses, were refined as riding models ($C–H_{ar}$ = 0.93 Å, $C–H_{Me}$ = 0.96 Å) and assigned an isotropic thermal parameter of 1.2 that of the bonded atoms. The asymmetric unit consists of one complex cation and one (BF_4) counterion. This last is affected by disorder, two different sites being located by difference Fourier syntheses. Better convergence was obtained with occupancy factors of 0.8 and 0.2, respectively. Refinement was pursued with restraints and the minor position was refined isotropically. The final conventional R factor was 0.068 for 3244 data, 20 restraints and 398 parameters, and 0.11 for all data, $wR(F^2)$ = 0.19, $w = 1/[\sigma^2(F_0^2) + (0.1126\ P)^2 + 0.27\ P]$ where $P = (F_0^2 + 2F_c^2)/3$. The largest difference peak and hole are respectively 0.59 and −0.045 eÅ^3.

CCDC reference number 154547. See http://www.rsc.org/suppdata/nj/b1/b102520c/ for crystallographic data in CIF or other electronic format.

Results and discussion

Ligand **L** was prepared by lithiation of 6,6′-dimethyl-2,2′-bipyridine with lithium diisopropylamine (LDA) at low temperature, followed by reaction with dichlorophenylphosphine. Subsequent oxidation with sodium periodate under phase transfer conditions provide the target ligand **L** in fair yield. The synthesis of **L** is summarised in Scheme 1.

The analytical and spectroscopic characteristics are consistent with the proposed structure. The P=O function was evi-

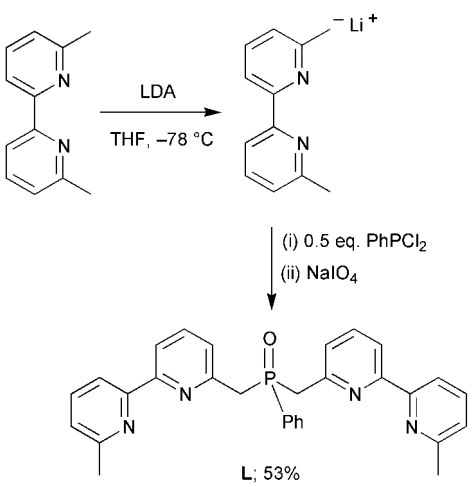

Scheme1

denced by IR spectroscopy at $\nu_{(P=O)} = 1185\ cm^{-1}$ and the presence of a phosphorus(v) atom was confirmed by a singlet at 36.5 ppm in the $^{31}P\{^1H\}$ NMR spectrum and a doublet for the geminal carbon at 40.9 ppm with $^1J_{PC} = 62$ Hz in the $^{13}C\{^1H\}$ NMR spectrum. The ^1H NMR spectrum of **L** displays, as expected, an $(AB)_2X$ (A = B = H, X = P) system at 3.86 ppm ($J_{AB} = J_{AX} = J_{BX} = 14.5$ Hz) for the two CH_2 protons.

Reaction of **L** with an equimolar amount of $[Cu(CH_3CN)_4](BF_4)$ in a mixture of acetonitrile and dichloromethane, under anaerobic conditions, led to the formation of a deep-red mononuclear complex. Single crystals, suitable for X-ray diffraction, were obtained after multiple recrystallisations based on slow diffusion of pentane in an acetone solution of the complex. The crystal structure of the [Cu**L**](BF_4) complex has been resolved and shows the molecular structure to consist of discrete entities, evidencing a 1 : 1 ligand-to-metal stoichiometry. An ORTEP view of the complex is given in Fig. 1 and selected bond lengths and angles are given in Table 1.

The two bipyridine subunits are wrapped around a single Cu(I) cation. Each copper(I) cation is coordinated to four nitrogen atoms provided by the pyridine rings to give a distorted tetrahedral arrangement with a small bite angle of *ca.* 81°. Two sets of Cu–N bonds are found: [2.013(4), 2.028(4) Å] for the pyridine rings close to the P=O function and [2.045(4), 2.048(4) Å] for the pyridine rings bearing the methyl groups. The two bipyridine chelates are almost planar with a somewhat more pronounced dihedral angle between the two pyridine rings in one bipyridine [the angle between the pyridine rings containing N1A and N1B is 1.8(3)° while the other two containing N1C and N1D are tilted by 8.8(2)°]. The tilt angles of the mean plane belonging to the phenyl ring and the adjacent pyridine rings are 56.6(2)° for N1A, 58.4(4)° for N1B, 32.7(1)° for N1C and 41.5(1)° for N1D. The shortest intermolecular distance of 4.4 Å is found between the oxygen atoms of the P=O functions for the two centrosymmetrical subunits lying at [*x*, *y*, *z*] and [−*x*, 1 − *y*, 1 − *z*], as depicted in Fig. 2. The packing of the molecules in the centrosymmetrical cell is shown in Fig. 3 the individual molecules are aligned along the *a* axis. The shortest intermolecular distance within a single chain is of the order of 3.4 Å between the mean plane of two adjacent pyridine rings belonging to two neighbouring complexes. In view of the absence of any symmetry element in the individual complex, each complex is chiral, but the bulk of the material is a racemic mixture of both isomers.

The ^1H NMR spectrum of this complex in deuteriated chloroform displays a complicated pattern for the CH_2 protons attributed to an AA′BB′X spin system (A = B = H, X = P; Fig. 4). The non-equivalence of each proton in both CH_2 groups indicates the absence of any symmetry element in the complex, in perfect agreement with the solid state structure.

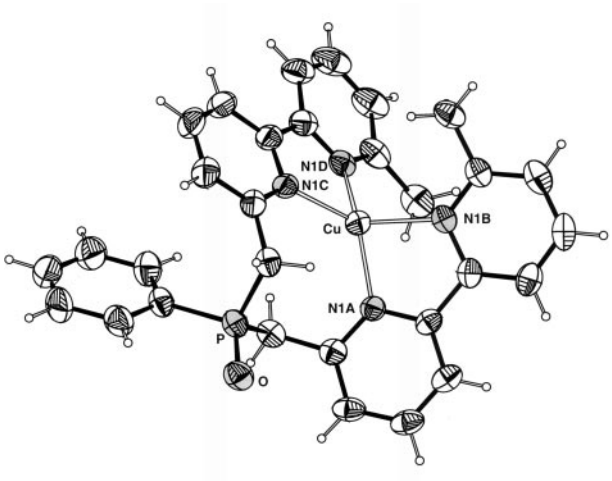

Fig. 1 ORTEP view of the [Cu**L**] cation. Displacement ellipsoids are shown at the 50% probability level.

Table 1 Selected bond lengths (Å) and angles (°) of the [Cu**L**](BF_4) complex

Cu–N1A	2.013(4)
Cu–N1C	2.028(4)
Cu–N1B	2.045(4)
Cu–N1D	2.048(4)
N1A–Cu–N1C	121.1(2)
N1A–Cu–N1B	81.5(2)
N1C–Cu–N1B	132.8(2)
N1A–Cu–N1D	139.2(2)
N1C–Cu–N1D	80.0(2)
N1B–Cu–N1D	109.3(2)

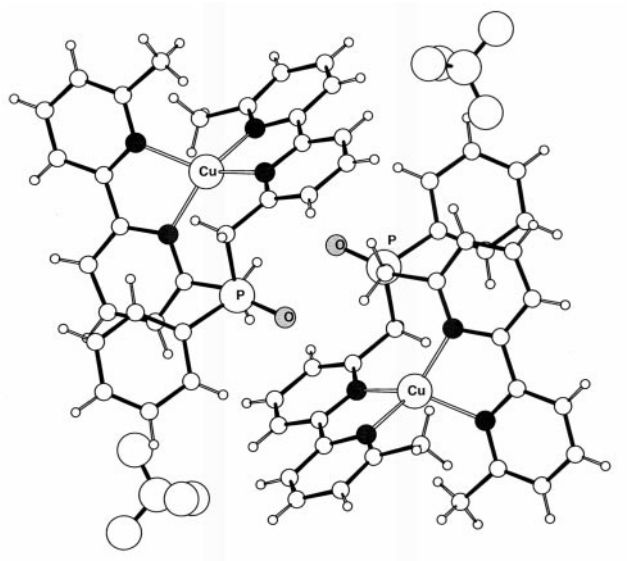

Fig. 2 Centrosymmetrical arrangement of two complexes within the crystallographic cell: (i) [*x*, *y*, *z*] and (ii) [−*x*, 1 − *y*, 1 − *z*]. Oi···Oii distance 4.398 (7) Å.

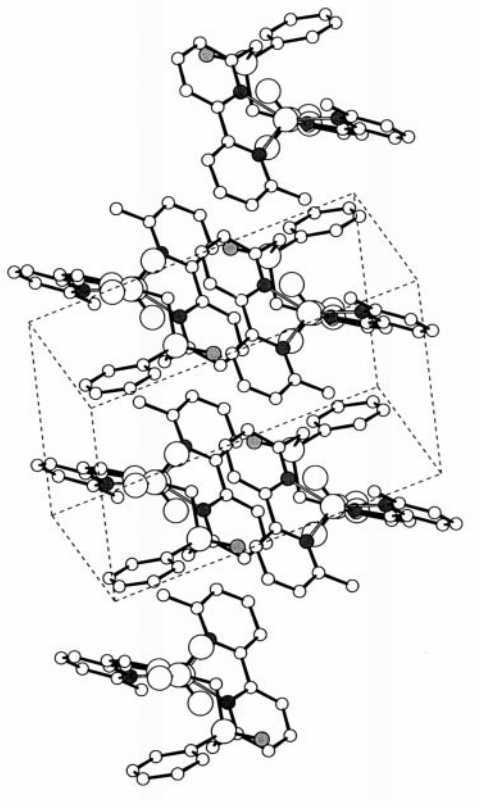

Fig. 3 Packing diagram over three crystallographic cells along the *a* axis.

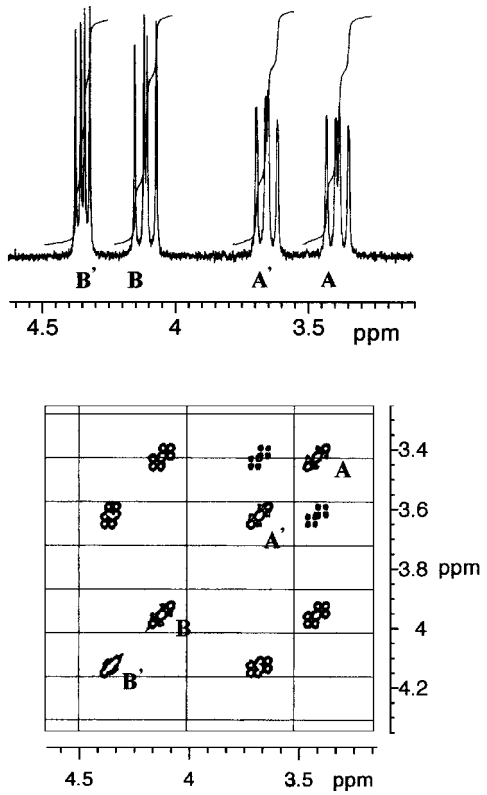

Fig. 4 (Top) Section of the ^{1}H NMR spectrum of the [Cu**L**](BF$_4$) complex in $CDCl_3$ showing the AA′BB′X spin system (A = B = H, X = P). (Bottom) 2D COSY NMR spectrum corresponding to the AA′BB′X spin system shown in the top half.

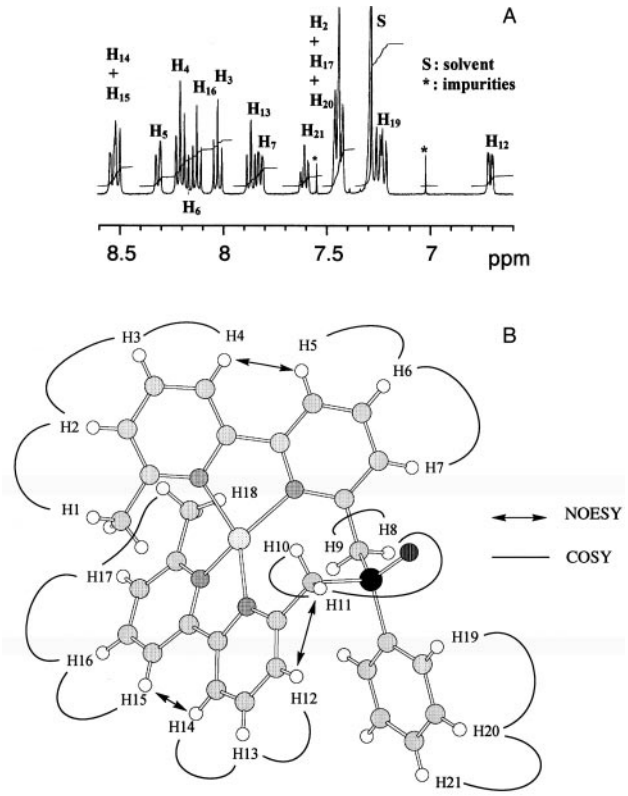

Fig. 5 (A) Section of the ^{1}H NMR spectrum of the [Cu**L**](BF$_4$) complex in $CDCl_3$ showing the aromatic part of the spectrum together with the labelling of the protons. (B) Molecular view of the complex with numbering of each proton with NOESY and COSY interaction pathways.

These data point to a differentiation of the two bipyridine moieties upon complexation with copper(I) and to the disappearance of the symmetry plane present in the free ligand.

The chemical shifts and some relevant coupling constants for this spin system are gathered in Table 2. From the 2D COSY NMR spectrum, a weak and long range coupling between the A parts of the AB systems ($^4J_{AA'} = 1$ Hz) can be seen (Fig. 4). The lack of any symmetry element in the complex is also evidenced by the presence of two singlets for the methyl groups at 1.89 and 1.92 ppm. These results unambiguously point to a slow interconversion process on the NMR timescale, with no chemical exchange between the two chiral forms of the complex.

From the chemical shifts, and 2D-COSY and NOESY experiments, the assignment of the protons of the ligand was possible (see Fig. 5 and Table 2). A first set of three signals corresponds to the five protons of the phenyl ring and were assigned in the following way: H19 at 7.23 ppm ($^3J_{PH} = 11.5$, $^3J_{HH} = 8$, $^4J_{HH} = 1.5$ Hz), H20 at 7.44 ppm ($^3J_{HH} = 8$ Hz) and H21 at 7.60 ppm ($^3J_{HH} = 8$ Hz). For the protons of the bipyridine arms, the assignment was achieved in two steps. In the first step, two families of 9 protons were separated. Starting from one of the singlets of the methyl substituent (the one at 1.89 ppm, for example) scalar correlations allowed for assignment of the protons on the adjacent pyridine ring (doublet at 7.44 ppm, triplet at 8.02 ppm and doublet at 8.21 ppm, respectively, for the protons in positions 5′, 4′ and 3′ of the pyridine ring of our example). A dipolar coupling between the protons in positions 3′ and 3 of this bipyridine gave the link between the two pyridine systems and the scalar couplings permitted the further assignment of the two remaining protons on this pyridine (doublet at 8.30 ppm, triplet at 8.18 ppm and doublet at 7.78 ppm, respectively, for the protons in positions 3, 4 and 5 in our example). Finally, the scalar correlations between the proton in the 5 position of the pyridine and the complicated spin system of the methylene bridges gave the resonances due to H_A and H_B (4.35 and 3.66 ppm, respectively, in our example). The same procedure applied to the second bipyridine arm allowed the assignment of the 9 remaining signals (Fig. 5). The second step involved the exact assignment of these two families of protons. This was achieved thanks to the observation of a considerable upfield shift of the doublet at 6.71 ppm, which was attributed to a proton at the 5 position of one of the bipyridine moieties (H7 or H12). On the basis of the X-ray crystal structure determination previously discussed, it appears that one of these protons [H12 in Fig. 5(B)] is located in the shielding region of the phenyl ring, highlighting the influence of the ring current, a phenomenon that has already been observed in numerous extended aromatic systems.[21] Assignment of H12 combined with the first step-by-step assignment of the protons of the bipyridine moieties gave the total assignment. From these results it appears that the weak ^4J coupling observed between H8 and H11 in the AA′BB′X spin system is perfectly in accord with the W-shaped

Table 2 Chemical shifts and relevant coupling constants for the ^{1}H NMR spectrum of [Cu**L**](BF$_4$) in $CDCl_3$; for atom labelling see Fig. 5(B)

Phenyl ring	H19	7.23		
	H20	7.44		
	H21	7.60		
Bipyridine moities	H1	1.89	H18	1.92
	H2	7.42	H17	7.44
	H3	8.02	H16	8.12
	H4	8.21	H15	8.50
	H5	8.30	H14	8.52
	H6	8.18	H13	7.86
	H7	7.78	H12	6.71
	H8	3.66 ($^2J_{HH} = 14$, $^2J_{PH} = 8$ Hz)	H11	3.40 ($^2J_{HH} = 14$, $^2J_{PH} = 18.5$ Hz)
	H9	4.35 ($^2J_{HH} = 14$, $^2J_{PH} = 18.5$ Hz)	H10	4.12 ($^2J_{HH} = 14$, $^2J_{PH} = 18.5$ Hz)

arrangement of the H8–C–P–C–H11 frame. This shape is observed in the solid state structure and is highly favourable for the observation of such long-range coupling.[22]

Finally, an important aspect of the NOESY experiment is the observation of exchange peaks between H7 and H12, H6 and H13, H5 and H14, H4 and H15 and H3 and H16. These exchange processes are observed as a result of a transfer of saturation between the interchanging sites.[22,23] From this observation, it can be estimated that the exchange process occurs at a rate at least equal to the inverse of the longitudinal relaxation time (T_1) of the aromatic protons, that is, of the order of a second.[22,24] Very interestingly, the 400 MHz ^{1}H NMR spectrum showed the two methyl signals to be separated by only 0.03 ppm. The separation of these peaks is only observable when the following requirement is fulfilled: $\tau \times \Delta\nu > 2\pi$, where τ is the time required for the observation of the distinct signals and $\Delta\nu$ the difference in frequency between the two observed signals. From this relation, one can conclude that the exchange process is shorter than $1/\tau$, which gives an upper limit of 75 s^{-1}. We can thus estimate that the rate of the interconversion process is situated in a window ranging from a few to 75 s^{-1}. Finally, the $^{31}P\{^1H\}$ NMR spectrum shows a singlet at 37.4 ppm in $CHCl_3$, in keeping with the observation that only the bipyridine moities of the ligand are complexed to the metal centre.

The electrochemical behaviour of [Cu**L**](BF_4) was studied by cyclic voltammetry in argon degassed acetonitrile solution at room temperature. Scanning anodically from 0.00 to +1.60 V *vs.* SCE, a single oxidation peak at +0.66 V is observed with a peak potential difference $\Delta E_p = E_{pa} - E_{pc}$ equal to 80 mV, which is independent of the scan rate between 10 and 1000 mV s^{-1}. The peak current increase linearly with $\omega^{1/2}$, which confirms an electron transfer mechanism without any chemical complication on the cyclic voltammetry time scale. This behaviour shows that the mononuclear copper(I) complex is oxidised in a reversible, monoelectronic diffusion-controlled step. Scanning cathodically from 0.00 to −2.00 V shows two successive reduction peaks at −1.60 and −1.84 V with a peak potential difference $\Delta E_p = E_{pc} - E_{pa}$ equal to 66 and 70 mV. Owing to the monoelectronic nature and reversibility of these two redox processes it is likely that they correspond to the successive reduction of the bipyridine ligands coordinated to the copper centre. It is expected that a metal-centred reduction providing Cu(0) should lead to an irreversible process accompanied by metallic copper deposition on the working electrode. It is surmised that ligand **L** provides excellent shielding of the cuprous centre and that the P(O)Ph subunit displays a significant withdrawing effect, which favours the successive reduction of each bipyridine subunit. This is further confirmed by the fact that [Cu(neocuproin)$_2$](BF_4)[25] (neocuproin = 2,9-dimethyl-1,10-phenanthroline) is substantially more difficult to reduce (by 120 mV) when studied under the same experimental conditions.

In order to gain a deeper insight into the mechanism of formation of this complex and to provide some information about stability constants, spectrophotometric titrations have been carried out in acetonitrile solutions containing 10^{-3} M of [(n-Bu)$_4$N](PF_6) as inert salt. Upon addition of the first aliquots of Cu^+, the colourless solution rapidly turned red as a result of a fast complexation process. For M/L ratios increasing from 0 to 1 (Fig. 6), the $\pi \rightarrow \pi^*$ transition centred at 291 nm for the free ligand is gradually shifted to lower energy with concomitant appearance of an absorption band in the visible region (λ_{max} = 420 nm), typical of an MLCT transition in Cu^+–bis(diimine) complexes.[26] At higher M/L ratio values, further changes are observed in the $\pi \rightarrow \pi^*$ region, but less pronounced than the previous one. Interestingly, the absorption band in the visible region remained essentially unchanged. Factorial analysis of the data revealed the formation of two distinct new absorbing species and an evolving factor analysis suggested a concentration maximum for the first species at an M/L ratio of 1, the second species appearing only for larger values. The titration was then fitted to the following model using the Spectfit software.[27]

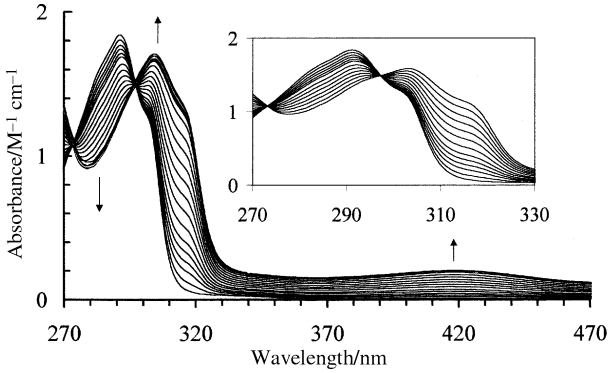

Fig. 6 Evolution of the UV-Vis absorption spectrum of a solution of **L** upon addition of increasing amounts of Cu^+ ([Cu^+]/[**L**] = 0 to 3 in CH_3CN with 10^{-3} M TBAPF_6). Inset: UV part of the absorption spectrum obtained with increasing amounts of Cu^+ from 0 to 1 equiv. *vs.* **L**.

$$Cu^+ + L \rightleftharpoons [CuL]^+ \beta_{ML} = [CuL]/([Cu^+][L])$$

$$2Cu^+ + L \rightleftharpoons [Cu_2L]^{2+} \beta_{M_2L} = [Cu_2L]/([Cu^+]^2[L])$$

Least squares fitting of the data to this model converges to values of 7.5 ± 0.5 and 13.1 ± 0.7 for log β_{ML} and log β_{M_2L}, respectively. The evolution of the concentrations of the species as a function of the M/L ratio (Fig. 7) confirmed the presence of the 1 : 1 complex as the major species (85%) at M/L ≈ 1.

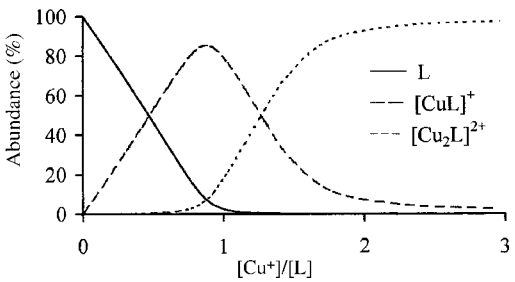

Fig. 7 Calculated evolution of the concentration of the species formed in solution as a function of the [Cu^+]/[**L**] ratio. The total ligand concentration is 7.0 × 10^{-5} M.

It is interesting to note that the second species formed still displays an absorption band in the visible region. This point indicates that the coordination of the second Cu^+ cation does not change the coordination of the two diimines around the first Cu^+ centre, as would be expected if the two metal atoms were each coordinated to one bipyridine arm (form **A**). In this last case, disappearance of the MLCT transition in the visible region would certainly be expected.[28] A possible explanation is the coordination of the second metal to the oxygen atom of the phosphine oxide moiety (form **B**), which is consistent with the pronounced perturbations in the UV domain associated with variations in the $\pi \rightarrow \pi^*$ transitions of the phenyl group.

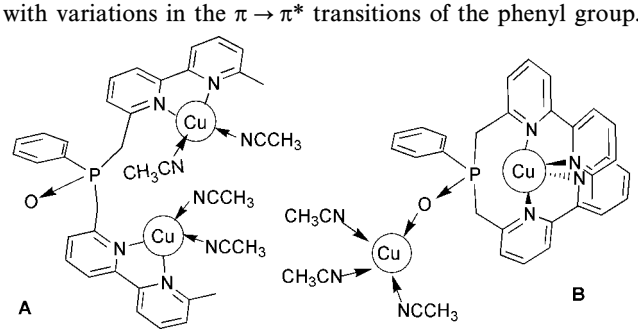

A set of additional experiments by phosphorous NMR in solution and FT-IR in the solid state support the possible coordination of a second cation to the mononuclear complex in the presence of a large excess of the metal precursor. Specifically, addition of 2 equiv. of $[Cu(CH_3CN)_4]^+$ to a solution containing [Cu**L**](BF_4) in CD_3CN under argon shows a significant downfield shift of the original singlet of 3.4 ppm with an enlargement of the peak (full width at half height = 1900 Hz) due to a dynamic process. Unfortunately, it was not possible to follow the evolution of the P=O stretching vibration in the IR spectrum, as a consequence of the superimposition of this band with the intense absorption due to the BF_4^- counteranion at 1053 cm^{-1}.[29] All these results indicate that at least in acetonitrile and in the presence of an excess of copper(I), additional copper coordination to the appended P=O function is possible. Further attempts to isolate and to structurally characterise this dinuclear complex have failed up to now.

Finally, it is worth pointing out that the copper-induced coordination of the bipyridine subunits does not result in a helicoidal arrangement as previously observed with more flexible frameworks. Molecular simulations using MM2 or PM3 programs seem to confirm that the dimers (helicate or meso-helicate) are less stable than the monomeric complexes. Stereoelectronic effects could be postulated to play a major role in the formation of the mononuclear *vs.* the dimeric complex. Similar observations were recently made with ferrocene-bridged bis(bipyridine) compounds.[30]

The UV-Vis absorption spectrum of [Cu**L**](BF_4) in acetonitrile (Fig. 8) displays two intense absorption bands in the UV domain. The first, with maximum at 263 nm (ε = 25 700 M^{-1} cm^{-1}) was attributed to $\pi \rightarrow \pi^*$ transitions on the phenyl ring, while the second band at 305 nm (ε = 27 100 M^{-1} cm^{-1}, with a shoulder on the low energy tail) was ascribed to $\pi \rightarrow \pi^*$ transitions on the bipyridine moieties. The visible part of the spectrum is dominated by two other transitions with maxima at 418 nm (ε = 3420 M^{-1} cm^{-1}) and 509 nm (ε = 1940 M^{-1} cm^{-1}). On the basis of their molar absorption coefficients and according to literature data,[25,26] these transitions can safely be assigned to MLCT transitions, as observed in numerous $[Cu(diimine)_2]^+$ complexes. The two transitions may be related to electron donation from the Cu^+ atom to two different bipyridine subunits, although the energy difference of the absorption maxima (0.54 eV) is substantially larger than the value observed by electrochemistry for the reduction of these two distinct bipyridines (0.24 eV). Finally, the title compound does not exhibit an intense steady-state emission at room temperature and in solution, in contrast with other copper(I) complexes bearing bulky phenanthroline ligands.[31]

Conclusion

The present system based on a bis-bipyridine/phosphine oxide ligand is significantly more rigid than those traditionally used to generate metallo-helicates and an important finding to emerge from this study is that a mononuclear complex is preferentially formed. An interesting aspect of this work, however, concerns the relatively high association constant determined by spectrophotometric titrations but also the discovery that in the presence of excess metal precursor a dinuclear complex is formed. It is surmised that within this complex the P=O fragment coordinates to the second copper(I) centre, a situation that could be favoured by the π-acidic character of the bipyridine fragments.

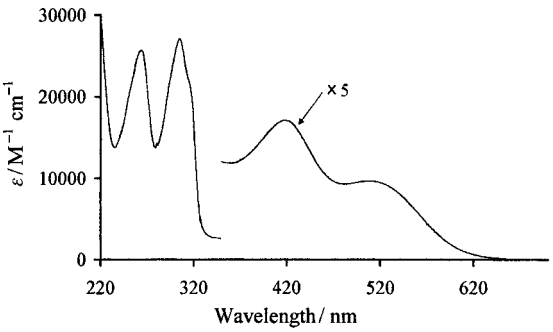

Fig. 8 UV-Vis absorption spectrum of [Cu**L**](BF_4) in acetonitrile.

Acknowledgements

This work was supported by the Centre National de la Recherche Scientifique and by the Engineering School of Chemistry (ECPM), We thank Dr Arlette Cavallo-Solladié for computational simulations and Dr Michel Schmitt for the COSY and NOESY NMR measurements.

References

1 M. Munakama, L. P. Wu and T. Kuroda-Sowa, *Adv. Inorg. Chem.*, 1999, **46**, 173.
2 C. L. Hill and X. Zhang, *Nature* (*London*), 1995, **373**, 324.
3 A. El-ghayoury, L. Douce, A. Skoulios and R. Ziessel, *Angew. Chem., Int. Ed.*, 1998, **37**, 2205.
4 C. P. Collier, E. W. Wong, M. Belohradsky, F. M. Raymo, J. F. Stoddart, P. J. Kuekes, R. S. Williams and J. R. Heath, *Science*, 1999, **285**, 391; C. P. Collier, G. Mattersteig, E. W. Wong, Y. Luo, K. Kristen, J. Sampaio, F. M. Raymo, J. F. Stoddart and J. R. Heath, *Science*, 2000, **289**, 1172.
5 C. Piguet, *J. Inclusion Phenom. Macrocyclic Chem.*, 1999, **34**, 361.
6 B. Olenyuk, A. Fechtenkötter and P. J. Stang, *J. Chem. Soc., Dalton Trans.*, 1998, 1707.
7 O. Mamula, A. Von Zelewsky and G. Bernardinelli, *Angew. Chem., Int. Ed.*, 1998, **37**, 290.
8 J.-P. Sauvage, *Acc. Chem. Res.*, 1998, **31**, 611; C. Kaes, A. Katz and M. W. Hosseini, *Chem. Rev.*, 2000, **100**, 3553.
9 J. M. Lehn, A. Rigault, J. Siegel, J. Harrowfiled and D. Moran, *Proc. Natl. Acad. Sci. U.S.A.*, 1987, **84**, 2565; J.-M. Lehn and A. Rigault, *Angew. Chem., Int. Ed.*, 1998, **27**, 1095; U. Koert, M. M. Harding and J. M. Lehn, *Nature* (*London*), 1990, **346**, 339.
10 E. C. Constable and M. D. Ward, *J. Am. Chem. Soc.*, 1990, **112**, 1256; E. C. Constable, M. D. B. Drew and M. D. Ward, *Chem. Commun.*, 1997, 1600; M. Borley, E. C. Constable, S. A. Corr, M. D. B. Drew and M. D. Ward, *Chem. Commun.*, 1998, 2665.
11 R. Ziessel, A. Harriman, J. Suffert, M.-T. Youinou, A. De Cian and J. Fischer, *Angew. Chem., Int. Ed. Engl.*, 1997, **36**, 2509.
12 R. Ziessel, L. Toupet, S. Chardon-Noblat, A. Deronzier and D. Matt, *J. Chem. Soc., Dalton Trans.*, 1997, 3777.
13 E. Psillakis, J. C. McCleverty and M. D. Ward, *J. Chem. Soc., Dalton Trans.*, 1997, 1645; J. S. Fleming, E. Psillakis, J. C. Jeffery, K. L. V. Mann, J. C. McCleverty and M. D. Ward, *Polyhedron*, 1998, **17**, 1705.
14 L. J. Charbonnière, C. Balsiger, K. J. Schenk and J.-C. G. Bünzli, *J. Chem. Soc., Dalton Trans.*, 1998, 505.
15 M. Tiecco, L. Testaferri, M. Tingoli, D. Chianelli and M. Montanucci, *Synthesis*, 1984, 736.
16 B. J. Hathaway, D. G. Holah and J. D. Poslethwaite, *J. Chem. Soc.*, 1961, 3215.
17 Kappa-CCD Software, Enraf–Nonius, Delft, The Netherlands, 1997.
18 Z. Otwinowski and W. Minor, *Methods Enzymol.*, 1997, **276**, 307.
19 G. M. Sheldrick, *Acta Crystallogr., Sect A*, 1990, **46**, 467.
20 G. M. Sheldrick, SHELXL-93, Program for the Refinement of Crystal Structures, University of Göttingen, Germany, 1993.
21 C. Piguet, G. Bernardinelli, B. Bocquet, A. Quattropani and A. F. Williams, *J. Am. Chem. Soc.*, 1992, **114**, 7440; L. J. Charbonnière, G. Bernardinelli, C. Piguet, A. M. Sargeson and A. F. Williams, *J. Chem. Soc , Chem. Commun.*, 1994, 1419.
22 H. Günther, *La Spectroscopie de RMN*, editions Masson, Paris, 1993.
23 J. K. M. Sanders and B. K. Hunter, in *Modern NMR Spectroscopy*, 2nd edn., Oxford University Press, Oxford, 1991, p. 222–234.
24 J.-M. Lehn and R. Ziessel, *Helv. Chim. Acta*, 1988, **71**, 1511.
25 R. M. Everly, R. Ziessel, J. Suffert and D. R. McMillin, *Inorg. Chem.*, 1991, **30**, 559 and references cited therein.
26 A. Juris and R. Ziessel, *Inorg. Chim. Acta*, 1994, **225**, 251.

27 H. Gampp, M. Maeder, C. J. Meyer and A. D. Zuberbühler, *Talanta*, 1985, **32**, 257.
28 M. Munakata, M. Maekawa, S. Kitagawa, S. Matsuyama and H. Masuda, *Inorg. Chem.*, 1989, **28**, 4300.
29 K. Nakamoto, *Infrared and Raman Spectra of Inorganic and Coordination Compounds*, 4th edn., Wiley, New York, 1986.
30 M. Buda, J.-C. Moutet, E. Saint-Aman, A. De Cian, J. Fischer and R. Ziessel, *Inorg. Chem.*, 1998, **37**, 4146.
31 C. O. Dietrich-Buchecker, P. A. Marnot, J.-P. Sauvage, J. R. Kirchhoff and D. R. McMillin, *J. Chem. Soc., Chem. Commun.*, 1983, 513.